Evidence for Pre- and Post-Power Stroke of Cross-Bridges of Contracting Skeletal Myofibrils

K. Midde,[†‡] R. Luchowski,[†‡‖] H. K. Das,[§¶] J. Fedorick,[†‡] V. Dumka,[†‡] I. Gryczynski,[†‡] Z. Gryczynski,[†‡] and J. Borejdo[†‡*]

[†]Department of Molecular Biology and Immunology, [‡]Center for Commercialization of Fluorescence Technologies, [§]Department of Pharmacology and Neuroscience, and [¶]Institute of Cancer Research, University of North Texas Health Science Center, Fort Worth, Texas; and [‖]Department of Physics, Maria Curie-Sklodowska University, Lublin, Poland

ABSTRACT We examined the orientational fluctuations of a small number of myosin molecules (approximately three) in working skeletal muscle myofibrils. Myosin light chain 1 (LC1) was labeled with a fluorescent dye and exchanged with the native LC1 of skeletal muscle myofibrils cross-linked with 1-ethyl-3-[3(dimethylamino) propyl] carbodiimide to prevent shortening. We observed a small volume within the A-band (~10^{-15} L) by confocal microscopy, and measured cyclic fluctuations in the orientation of the myosin neck (containing LC1) by recording the parallel and perpendicular components of fluorescent light emitted by the fluorescently labeled myosin LC1. Histograms of orientational fluctuations from fluorescent molecules in rigor were represented by a single Gaussian distribution. In contrast, histograms from contracting muscles were best fit by at least two Gaussians. These results provide direct evidence that cross-bridges in working skeletal muscle assume two distinct conformations, presumably corresponding to the pre- and post-power-stroke states.

INTRODUCTION

Muscle contraction results from the cyclic interaction of myosin heads with actin filaments. A critical intermediate step in this cycle is the power stroke, a conformational change in myosin that causes force production and/or sliding of myosin-containing filaments relative to actin-containing filaments. The biochemistry of the actomyosin interaction is well understood (1–4) and implies that the formation of a pre-power-stroke state results from the binding of myosin-containing hydrolytic products to actin. The release of phosphate causes a force-generating conformational change of the bound head that leads to the formation of a post-power-stroke state. In this state, both ADP and actin are bound to a myosin head (ADP is bound weakly, hence the term "weak ADP binding state" (5)). Dissociation of ADP transforms this state to a rigor conformation in which myosin, devoid of hydrolytic products, binds strongly to actin. The conformation of a cross-bridge in a weak ADP binding state is nearly the same as in rigor. After that, the cross-bridge enters the so-called near-rigor state, in which a head is still bound to actin but allows ATP binding. Release of ADP causes the head to bind to a new ATP molecule and thus detach from actin and hydrolyze ATP (6). The pre-power-stroke and post-power-stroke states are also known as closed and open states, respectively (1). In this work we examine the distribution of cross-bridges between the pre- and post-power-stroke states of the myosin ATPase cycle.

Strong evidence for the existence of distinct pre- and post-power-stroke states has been provided by in vitro single-molecule (7), crystallography (5), and electron microscopy (8) studies of the processive myosin V molecule. Earlier, elegant EPR studies (9) suggested the existence of three structural states of myosin II in working muscle fibers. One state, the rigor state, has been well characterized in ex vivo muscle. This conformation has been extensively described, because all of the cross-bridges in rigor are immobile and assume a well-defined orientation with respect to the muscle axis (10–12). Investigators have obtained valuable information about cross-bridge orientation, number, position, and angle in actin target zones by measuring large assemblies of cross-bridges in insect flight (13) and vertebrate skeletal muscle (9,12,14–17). In this work, we are specifically interested in the distribution of cross-bridge orientations during contraction. Because cross-bridges act asynchronously during contraction, the resulting information about spatial distribution is not very useful if it is averaged over many molecules. Therefore, it is necessary to examine a distribution of cross-bridge fluctuations about the average value, i.e., to follow the motion of mesoscopic (affected by fluctuations around the average (18)) of myosin molecules. The size of the fluctuation is inversely proportional to the number of molecules under study, and therefore we looked at very small assemblies of cross-bridges (three to four molecules) in isometrically contracting skeletal muscle myofibrils.

The method applied in this study is based on the ability to observe a few molecules of myosin in an ex vivo muscle, as illustrated in Fig. 1. Muscle myosin light chain 1 (LC1) is labeled with rhodamine and exchanged with native LC1 of a myofibril. A small volume within labeled muscle (10^{-16} L) is illuminated by a focused laser beam (Fig. 1, *green hourglass*), and the fluorescence is observed by confocal microscopy. The detection volume (DV; *dashed line*) of the microscope is an ellipsoid of revolution whose

Submitted August 18, 2010, and accepted for publication January 5, 2011.

*Correspondence: Julian.Borejdo@unthsc.edu

Editor: Christopher Lewis Berger.

0006-3495/11/02/1024/10 $2.00

doi: 10.1016/j.bpj.2011.01.007

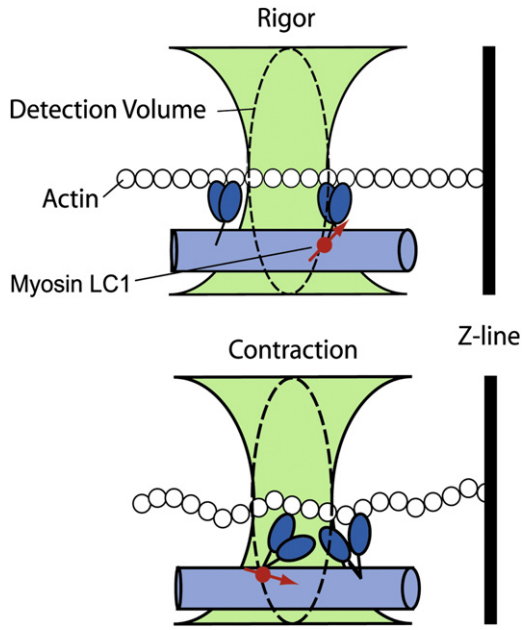

FIGURE 1 Origin of fluorescence fluctuations. A small fraction of myosin within the myofibril is bound to rhodamine-labeled LC1 (*red circle*). In rigor (*top panel*) there are no fluctuations in the orientation of the fluorophore's transition dipole (*red arrow*). During contraction (*bottom panel*) the myosin cross-bridges are cycling, which changes the orientation of the rhodamine's transition dipole and causes fluctuations of polarized intensity. We measure fluctuations in dipole orientation by recording parallel ($\|$) and perpendicular ($\perp$) components of the emitted fluorescent intensity by the cross-bridge-bound fluorophores.

small diagonal measures 1.2 μm. If the degree of labeling is sufficiently small, this volume will contain three to four fluorescent molecules of myosin (see the "Number of observed molecules" section in the Results). In rigor muscle (*top panel*), the myosin cross-bridges are stationary and no fluctuations in the orientation of the transition dipole occur. During contraction, on the other hand, the myosin cross-bridges undergo power-stroke cycles (*bottom panel*). The power stroke changes the orientation of a transition dipole of rhodamine attached to LC1, i.e., the orientation of rhodamine dipole fluctuates in time. We measured these fluctuations by simultaneously recording parallel ($I_{\|}$) and perpendicular ($I_{\perp}$) components of fluorescent light emitted by a myosin-bound fluorophore. Each of these components reflects orientational changes of the myosin head C-terminus. The normalized difference between these components, i.e., the polarized fluorescence (P), is a sensitive indicator of the orientation of the transition dipole of the fluorophore (15,19–25). We performed an elementary statistical analysis to analyze the observed fluctuations, and found that the fluctuations of the rigor muscles were distributed according to a single Gaussian distribution. In contrast, the histograms of contracting muscles could be fitted by at least two Gaussians. This provides evidence that cross-bridges in working skeletal muscle assume two distinct conformations, presumably corresponding to the pre-and post-power stroke states of the myosin ATPase cycle.

MATERIALS AND METHODS

Chemicals and solutions

Tetramethylrhodamine-5-iodoacetamide dihydroiodide (5-TMRIA, single isomer) was purchased from Molecular Probes (Eugene, OR; Cat. No. T-6006). All other chemicals were obtained from Sigma-Aldrich (St. Louis, MO). The composition of the solutions was identical to that used by Muthu et al. (26).

LC1 expression

A pQE60 vector containing recombinant LC1 with a single cysteine residue (Cys-178) was donated by Dr. Susan Lowey (University of Vermont). The plasmid DNA was transformed into *Escherichia coli* M15 competent cells, and recombinant clones were selected by ampicillin resistance. The LC1-cDNA insert of the clones was confirmed by DNA sequencing of both strands (Iowa State University of Science and Technology). LC1 protein was overexpressed in Luria broth containing 100 μg/ml of ampicillin by induction with IPTG. His-tagged LC1 protein was affinity-purified on a Ni-NTA column according to the manufacturer's protocol. The imidazole-eluted fractions were run on SDS-PAGE followed by Western analysis with Anti-LCN1 antibodies (Abcam, Cambridge, MA). Fractions containing LC1 were pooled together and dialyzed with buffer (50 mM KCl and 10 mM phosphate buffer, pH 7.0). Dialyzed protein showed a single ~25-kDa band on SDS-PAGE after Coomassie staining (see Fig. S1 in the Supporting Material). Protein concentration was determined by using the Bradford assay.

LC1 labeling

Purified LC1 was dialyzed against buffer A (50 mM KCL and 10 mM phosphate buffer, pH 7.0) and fluorescently labeled by incubation with a 5 molar excess of 5-TMRIA for 6 h in buffer A on ice. To eliminate unbound dye, the solution was passed through a Sephadex G50 column.

Degree of labeling of LC1

The concentrations of LC1 protein and bound 5-TMRIA were determined to estimate the degree of labeling. Protein concentration was determined by the Bradford assay, and 5-TMRIA concentration was determined from the peak absorbance ($\varepsilon = 87{,}000\ M^{-1}cm^{-1}$ at 535 nm) obtained on a Varian Eclipse spectrometer (Varian, Palo Alto, CA). The concentrations of the protein and 5-TMRIA dye were found to be the same, indicating that the dye and protein were bound in a 1:1 ratio.

Preparation of myofibrils

Rabbit psoas muscle bundles were washed with an ice-cold EDTA-rigor solution (50 mM KCl, 5 mM EDTA, 10 mM TRIS-HCl, pH 7.5) for 0.5 h, followed by an extensive washing with Mg^{2+}-rigor solution (50 mM KCl, 2 mM $MgCl_2$, 10 mM TRIS-HCl, pH 7.5) and then with Ca^{2+}-rigor solution (50 mM KCl, 0.1 mM $CaCl_2$, 10 mM TRIS-HCl, pH 7.5). The fiber bundle was then homogenized with the use of a Heidolph Silent Crusher S homogenizer for 20 s (with a break to cool after 10 s) in Mg^{2+}-rigor solution.

LC1 exchange into myofibrils

Fluorescently tagged LC1 (R-LC1) was incubated with 1 mg/ml of freshly prepared myofibrils in light-chain exchange solution (15 mM KCl, 5 mM EDTA, 5 mM DTT, 10 mM KH_2PO_4, 5 mM ATP, 1 mM TFP, and 10 mM imidazole, pH 7) for 5 min at 30°C (12). The concentration of R-LC1 was 3 nM unless otherwise specified.

Probability distribution measurements

Fluorescence fluctuations were acquired on an Alba-FCS confocal system (ISS, Urbana, IL) coupled to an Olympus IX 71 microscope. The experimental arrangement was the same as that previously described by Borejdo et al. (27). In brief, excitation was provided by a 532 nm CW laser. A polarizer was inserted before the entrance to the microscope to ensure that the exciting light was linearly polarized, and the resulting laser polarization was vertical with respect to the microscope stage. The confocal pinhole was 50 μm. The emitted fluorescent light was split by a prism, and each component was detected by a separate Avalanche PhotoDiode (APD) through $\parallel$ and $\perp$ oriented analyzers. Myofibrils were always placed with their long axis aligned vertically on the microscope stage. We collected 2 M data points every 10 μs for 20 s and smoothed the data by binning 1000 points. Before each experiment, the instrument was calibrated and optimized with a 50 nM solution of rhodamine G. Following the notation of Tregear and Mendelson (22), let ${}_{\parallel}I_{\perp}$ be the polarized intensity obtained with the exciting and detected light polarized parallel to the myofibril axis, and ${}_{\parallel}I_{\perp}$ be the polarized intensity obtained with exciting and detected light polarized parallel and perpendicular to the myofibril axis, respectively. Channel 1 (ch1) was used to detect ${}_{\parallel}I_{\perp}$, and channel 2 (ch2) was used to detect ${}_{\parallel}I_{\parallel}$. We calculated polarization as $({}_{\parallel}I_{\perp} - {}_{\parallel}I_{\parallel})/({}_{\parallel}I_{\perp} + {}_{\parallel}I_{\parallel})$. Thus, the reported polarization values are negative values of the conventional $P_{\parallel}$ polarization parameter.

Steady-state force measurements

A small bundle of skinned skeletal muscle fibers (two to five) from rabbit psoas were attached by tweezer clips to a force transducer (Scientific Instruments, Heidelberg, Germany). The fibers were stretched until taut in 1 ml of pCa 5 rigor solution (50 mM KCl, 0.1 mM $CaCl_2$, 10 mM TRIS-HCl, pH 7.5), and then a contracting solution (50 mM KCl, 0.1 mM $CaCl_2$, 5 mM MgATP, 10 mM TRIS-HCl, pH 7.5) was added to test for maximal steady-state force. We tested whether LC1 exchange modified the tension of the muscle fibers. Fibers were exchanged with 100 nM fluorescent LC1 at 30°C for different periods of time. In $N = 60$ experiments on different fibers, the average maximal force per unlabeled fiber was 1.6 $\pm$ 0.1 mN (mean $\pm$ SE). The force was also measured after exchange for 5 ($N = 6$), 10 ($N = 5$), 15 ($N = 8$), or 30 ($N = 6$) min. At 5 and 10 min after exchange, the force was unchanged. At 15 min, the force was actually increased to 1.9 mN/fiber and again decreased to the unlabeled value of 1.6 mN/fiber at 30 min. Because in our experiments the myofibils were exchanged for 5 min with 3 nM fluorescent LC1, we conclude that labeling has no effect on fiber tension or myofibril function.

Cross-linking

In the presence of Ca^{2+} and ATP, the myofibrils shortened, which made it impossible to record polarized intensities during contraction. Therefore, we prevented the myofibrils from shortening by cross-linking them with the water-soluble cross-linker 1-ethyl-3-[3-(dimethylamino)propyl]carbodiimide (EDC) (28,29). Myofibrils (1 mg/ml) in rigor solution (50 mM KCl, 20 mM EDC, 0.1 mM $CaCl_2$, 10 mM TRIS-HCl, pH 7.5) were incubated for 20 min at room temperature. The reaction was stopped by addition of 20 mM DTT. The pH of the solution (7.4) remained unchanged throughout the 20 min reaction. We verified the lack of shortening by imaging the myofibrils by differential contrast microscopy, and by fluorescence microscopy after labeling the myofibrils with 10 nM rhodamine-phalloidin (30).

Time-resolved anisotropy and lifetime measurements

We measured the fluorescence anisotropy and lifetimes using a time-domain technique and a FluoTime 200 fluorometer (PicoQuant, Berlin, Germany). The excitation was provided by a 475-nm pulsed diode laser, and the observation was conducted through a 590 nm monochromator with a supporting 590-nm long-pass filter. The full width at half-maximum of the pulse response function was 68 ps (measured by PicoQuant), and the time resolution was better than 10 ps. We analyzed the intensity decays in terms of a multiexponential model using FluoFit software (PicoQuant). All experiments were performed at room temperature (~23°C).

Statistical analysis

Statistical analysis was performed with the use of SigmaPlot 11.02 and PeakFit v. 4.12 (Systat, San Jose, CA) and Origin v. 8.5 (OriginLab, Northampton, MA) software. The quality of fit to either a single or double Gaussian function was assessed by the standard error (PeakFit, San Jose, CA) or reduced χ^2 (Origin) parameters.

RESULTS

Imaging

A typical fluorescence lifetime image of a rigor myofibril is shown in Fig. 2. All A-bands were fluorescently labeled. The red circle in Fig. 2 *A* indicates a two-dimensional projection of the confocal aperture on the image plane, and its diameter (1.2 μm) is equal to the diameter of the confocal aperture (50 μm) divided by the magnification of the objective (40×). Images are shown at various degrees

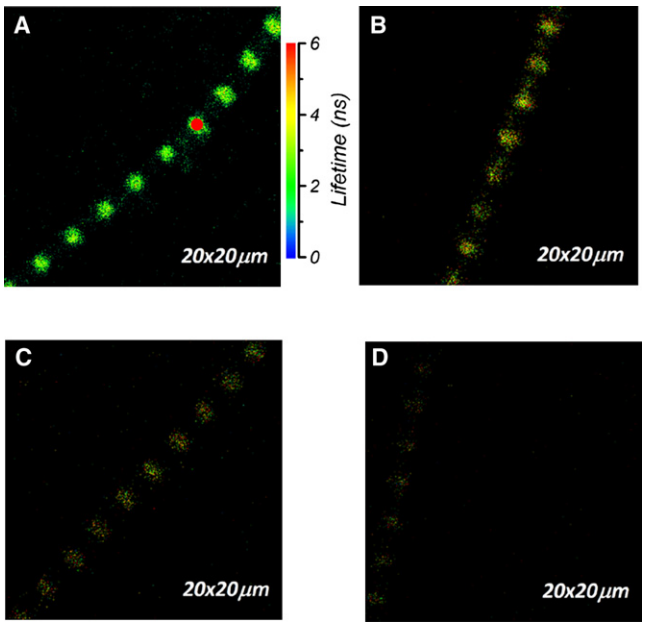

FIGURE 2 Lifetime images of a rigor myofibril. The color bar to the right of image *A* is the lifetime scale from 0 (*blue*) to 6 (*red*) ns. The red circle is a projection of the confocal aperture on the sample plane (diameter 1.2 μm). Native LC1 molecules were exchanged in myofibrils with 4 nM (*A*), 2 nM (*B*), 1.2 nM (*C*), and 0.8 nM (*D*) of R-LC1. Sarcomere length = 3.1 μm (*A*), 3.0 μm (*B*), 3.0 μm (*C*), and 2.9 μm (*D*). Images were acquired on a PicoQuant Micro Time 200 confocal lifetime microscope. The sample was excited with a 470 nm pulse of light and the emission was collected on an APD through a LP500 filter.

of labeling. Native LC1 of the myofibrils was exchanged with 4 nM (*A*), 2 nM (*B*), 1.2 nM (*C*), and 0.8 nM (*D*) of R-LC1. In the experiments reported here, the myofibrils were exchanged with 3 nM R-LC1.

LC1 is immobilized by the myosin neck

We measured the decay of anisotropy of R-LC1 exchanged into myofibrils to test whether rhodamine was rigidly immobilized on the surface of LC1. This was done to ensure that the orientation of the transition dipole of the fluorophore would reflect the orientation of the neck portion of the myosin head. Anisotropy is defined as $r = (I_{\parallel} - I_{\perp})/(I_{\parallel} + 2I_{\perp})$. (The decay is shown in Fig. 4.) The decay of free TMRIA was best fit by a double exponential curve $r(t) = Ro + a \times \exp(-t/\theta_1) + b \times \exp(-t/\theta_2)$, where Ro = 0.05 is the value of anisotropy at infinite time, and $\theta_1 = 0.3$ and $\theta_2 = 608.7$ ns are the rotational correlation times (Fig. 3 *A*). The fast decay accounted for most of the anisotropy decay (93.1%), and thus the slow correlation time accounted for only 6.9% of the decay, probably due to aggregates of rhodamine. The decay of R-LC1 bound to myofibrillar myosin was best fit by the same double exponential function, but this time Ro = 0.33, $\theta_1 = 67.7$, and $\theta_2 = 0.9$ ns (Fig. 3 *B*). The slow and fast correlation times accounted for 82.1% and 17.9%, respectively, of the decay. The short and long correlation times were most likely due to the rotation of the rhodamine moiety on LC1 and the rotation of bound LC1, respectively. The maximum value of anisotropy was 0.384, and this high value of initial anisotropy indicates that the absorption and emission dipoles of rhodamine are nearly parallel.

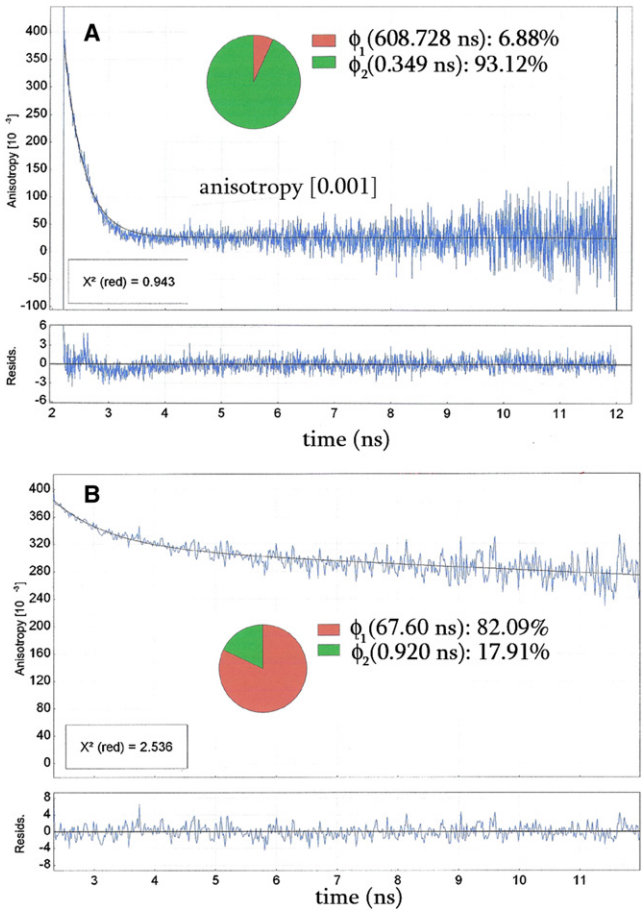

FIGURE 3 Anisotropy decay of 0.1 μM free TMRIA (*A*) and 50 μM myofibrils (*B*) after exchange with 2.5 μM R-LC1 into 1 mg/ml myofibrils for 5 min at 30°C.

Number of observed molecules

Because asynchronous operation of a large number of cross-bridges will average out any fluctuations, it is essential to make sure that the data are collected from only a few molecules. Therefore, we labeled the myosin very sparsely with fluorescent LC1 (myofibrils were incubated with 3 nM rhodamine-LC1) and then placed a myofibril in the focus of the microscope. To determine how many molecules contributed to the observed fluorescence, we measured the autocorrelation function (ACF) of fluorescence fluctuations for selected fluorophore concentrations. The value of the ACF at delay time 0 [G(0)] is equal to the inverse of the number of molecules *N* contributing to the signal, $N = 1/G(0)$ (31,32). The ACFs were obtained for solutions of TMRIA in the range of 1.7–8.5 nM. An example of the ACF obtained at a concentration of 6.8 nM is shown in Fig. 4 *A*. The value of G(0) was 0.07, giving an average number of molecules of ~14. The number of molecules estimated from the cross-correlation functions of ch1 and ch2 are plotted in Fig. 4 *B* as red and green circles, respectively. Extrapolation yields the approximate number of photons per one fluorophore as ~1400 counts/s per channel.

We were unable to obtain the ACFs at very low concentrations of the dye ($\leq$3.4 nM TMRIA) because the ACFs were simply too noisy. Therefore, we measured the intensity of the signal as a function of the concentration of the dye. The plot of concentration versus counts in ch1 and ch2 is shown in Fig. 4 *C*. The DV of the microscope is an ellipsoid of revolution whose waist (1.2 μm) is equal to the diameter of the confocal pinhole ($2\omega o$ = 50 μm) divided by the magnification of the objective (40×). The ellipsoid is assumed to have a waist ωo and height, zo, equal to the thickness (1 μm) of a typical myofibril. Therefore, DV = $4/3\pi\omega o^2 zo$ is ~1 μm^3. This is approximately equal to the volume of a typical half-sarcomere. Knowing the DV and concentration, we calculated the number of molecules in the DV. The concentration of 1.7 nM TMRIA corresponds to a single fluorophore. Extrapolation yields the approximate number of photons per one fluorophore: ~100 counts/s per channel. Averaging extrapolated values from Fig. 4, *B* and *C*, yields ~750 counts/s from a single fluorophore.

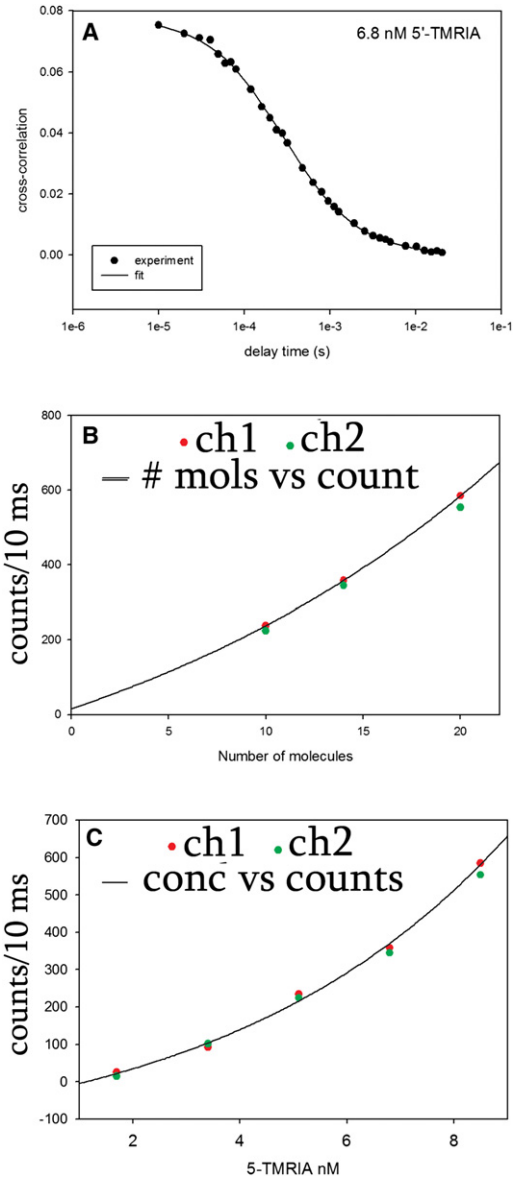

FIGURE 4 (*A*) Cross-correlation function of 6.8 nM TMRIA. The number of molecules in the DV was obtained from the inverse of the cross-correlation value extrapolated at a delay time equal to zero. (*B*) Plot of the number of molecules in the DV obtained from the inverse of cross-correlation function versus signal intensity for ch1 (*red dots*) and ch2 (*green dots*). The solid line is a single exponential, three-parameter fit ($y = yo + ab^x$). (*C*) Signal intensity plotted as a function of TMRIA concentration (1.7–8.5 nM) for ch1 (*red dots*) and ch2 (*green dots*). The solid line is a single exponential, three-parameter fit ($y = yo + ab^x$). The number of molecules in the DV at a TMRIA concentration of 1.7 nM corresponds to one molecule, and the number of photons per fluorophore in plots *B* and *C* was estimated to be ~750 counts/s per channel.

Intensity fluctuations during rigor and contraction of muscle myofibrils

A myofibril was placed on the stage of the confocal microscope with the long axis oriented vertically on the microscope stage. The linear polarization of the illuminating laser light was also vertical, i.e., parallel to the myofibrillar axis. The fluorescence emanating from the DV was split 50/50 by a beam splitter and projected through 50 μm confocal apertures onto the photosensitive surface of the two APDs. Fig. S2 shows a typical time course of polarized intensity of a rigor (*A*) and contracting (*B*) myofibril. The original data were collected every 10 μs, but to smooth data and to keep the files to a manageable size, we binned 1000 points together to obtain a time resolution of 10 ms. The vertical scale is the number of counts during 10 ms.

Estimation of the number of molecules contributing to the signal from the myofibril

The average intensities from contracting myofibrils in ch1 and ch2 were 21 and 23, respectively (Fig. S2). For rigor myofibrils, the averages were 23 and 27 counts/10 ms, respectively (note that Fig. S2 is a bar plot). Thus, the average (23 counts/10 ms) corresponds to 2300/750, or ~3 myosin molecules.

Skewness and kurtosis

Fig. 5 shows examples of six histograms of polarized fluorescence randomly selected from a pool of 20 histograms obtained from myofibrils in rigor. A histogram can be quantitatively characterized by the values of kurtosis and skewness. A positive skewness means that the tail of the curve is directed toward positive values of the histogram relative to a Gaussian distribution. This was the case for both rigor and contraction (see below). A positive kurtosis is expressed by long tails and higher peaks compared with the Gaussian curves. This was the case for rigor myofibrils. A negative kurtosis means that the tails are smaller than those of Gaussian curves. This was the case for contracting myofibrils (see below). Zero skewness and kurtosis means that the histograms are Gaussian. This was the case for the uncross-linked myofibrils in rigor. Table 1 shows the values of skewness and kurtosis. The differences in both skewness and kurtosis between EDC-rigor and contracting myofibrils were both statistically significant. The average values of skewness for rigor histograms were influenced by cross-linking. The difference was statistically significant.

Effect of EDC

We sought to ascertain whether cross-linking makes a difference in the rigor distribution. Fig. S3 of the shows a rigor distribution obtained from uncross-linked myofibrils. The goodness of fit, assessed by χ^2, showed that none of the curves were significantly improved by the addition of a second Gaussian. The second peak accounts for (clockwise, starting from upper left) 0, 6.4, 0, 0.3, 0, and 8.3% of the total signal (average = 2.5%). The average was even smaller in the remaining 12 experiments. Even though

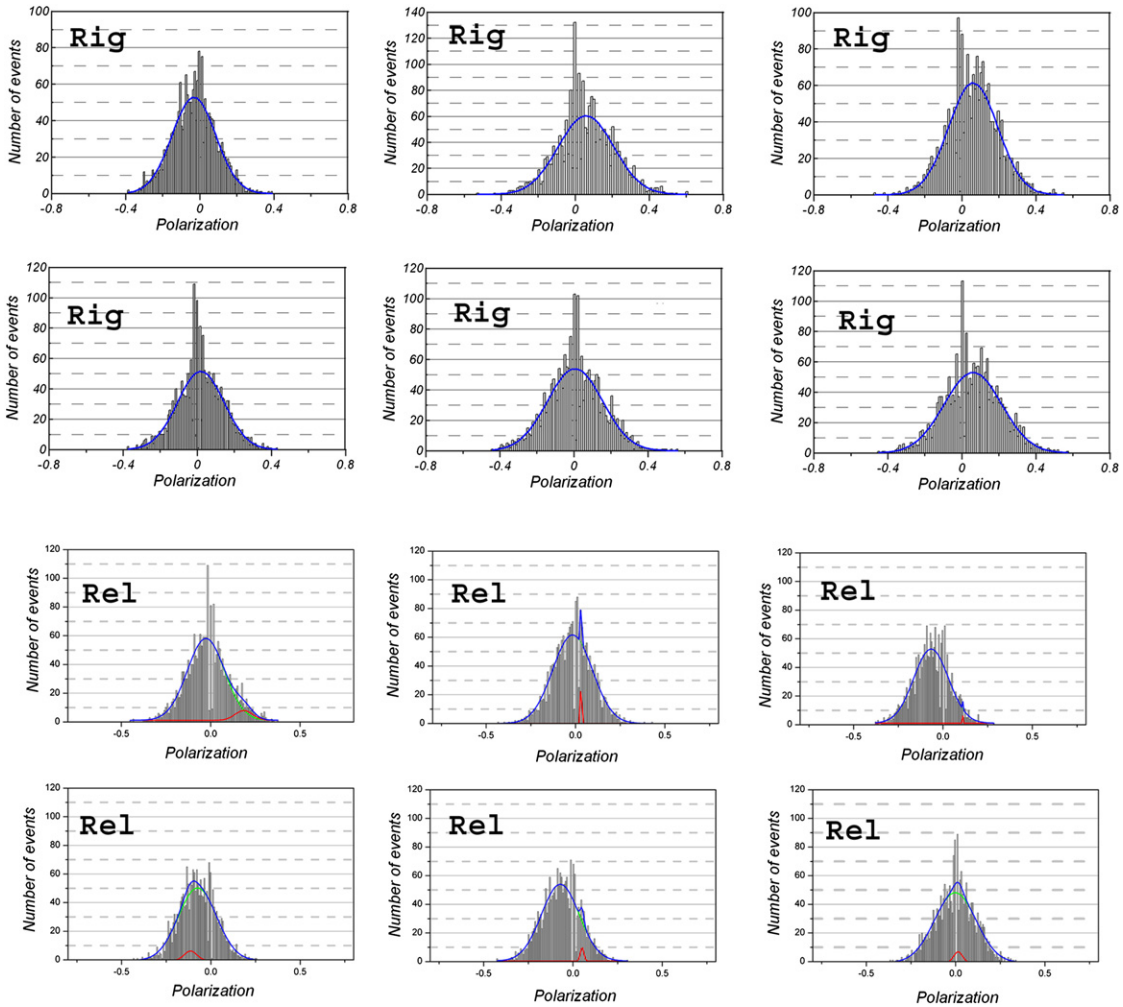

FIGURE 5 Examples of histograms of polarized fluorescence from rigor (*top panel*) and relaxed (*bottom panel*) myofibrils. Horizontal scale: The negative value of parallel fluorescence polarization. Vertical scale: The number of events during 20 s. The position of peaks for rigor myofibrils were (*top panel*, clockwise from the top left): P = −0.07, P = 0.05, P = 0.08, P = 0.02, P = 0.00, P = 0.07. The blue line shows the fit to a single Gaussian distribution. For relaxed myofibrils (*bottom panel*), the parameters (area, center, width, and height) for each peak of a two Gaussian fit are given in clockwise order, starting from the upper left. Upper left: minor peak (*red*) 0.85, 0.18, 0.10, 6.82; major peak (*green*) 14.89, −0.03, 0.21, 57.01. Upper middle: minor peak (*red*) 0.64, 0.03, 0.00, 115.88; major peak (*green*) 17.16, −0.02, 0.22, 61.66. Upper right: minor peak (*red*) 0.11, 0.11, 0, 86.96; major peak (*green*) 12.63, −0.07, 0.19, 51.74. Lower left: minor peak (*red*) 1.09, 0.05, 0.09, 10.09; major peak (*green*) 12.10, 0.09, 0.18, 53.36. Lower middle: minor peak (*red*) 0.23, 0.05, 0.02, 9.54; major peak (*green*) 14.24, −0.07, 0.21, 53.62. Lower right: minor peak (*red*) 0.47, 0.01, 0.05, 7.57; major peak (*green*) 14.30, −0.00, 0.23, 48.84. The contribution of the minor peak (*red line*) makes little difference relative to the second peak (*green line*) of a double Gaussian distribution fit. The blue line is the sum of red and green line fits.

the cross-linking is extensive (29), we believe that it makes no difference in terms of our conclusions in this study. Cross-linking occurs between myosin heads and actin, and between LMM tails, which are remote enough from LC1 to have no effect on the observed fluctuations.

Rigor histograms

The fit of representative histograms in rigor with a three-parameter Gaussian curve ($y = a \exp[-0.5(x - xo/b)^2]$) is shown in the top panel of Fig. 5 (*blue line*). The goodness of fit, assessed by standard error in the PeakFit program, showed that none of the curves were significantly improved by the addition of a second Gaussian. This point is illustrated in Fig. S4, which shows the two-Gaussian fit to the same data. The ratios of the areas under the major (*green*) and minor (*red*) peaks were (clockwise from upper left) 17.5, 18.1, 11.6, 59.5, 12.6, and 55.0, with an average of 29.0, indicating that adding the second Gaussian made on average only a 3.4% difference. The average position of a single peak was P = 0.05 ± 0.08 (in an oriented, immobile system, the fact that the polarization = 0 does not necessarily mean that the dipoles are randomly arranged). Because the absorption and emission dipoles of rhodamine are nearly parallel (time zero anisotropy ≈ 0.4; Fig. 3) and the myofibrillar axis is parallel to the direction of

TABLE 1 Comparison of kurtosis and skewness parameters from fluorescence polarization fluctuation histograms of rigor and contracting skeletal myofibrils

Myofibrils	Skewness	Kurtosis	*N*
Rigor	−0.02 ± 0.04	0.06 ± 0.18	18
EDC-rigor	1.12 ± 0.34	0.84 ± 1.63	18*
Relaxation	1.04 ± 0.19	0.20 ± 0.81	18
EDC-relaxation	1.48 ± 0.54	3.00 ± 3.05	18
Contraction	0.86 ± 0.16	−0.59 ± 0.27	18*

Errors are given as SD, and *N* is the number of experiments.
*Two histograms with extreme maxima and minima were rejected.

polarization of exciting light, this indicates that the transition dipoles of rhodamine in rigor are oriented mostly perpendicular to myofibrillar axis.

Relaxation histograms

Histograms of relaxed myofibrils were also best fit by a single Gaussian. The bottom panel of Fig. 5 shows the representative histograms during relaxation. The ratios of the areas under the major (*green*) and minor (*red*) peaks were (clockwise from upper left) 17.4, 26.8, 114.5, 12.0, 61.7, and 31.1, with an average of 43.9, indicating that adding the second Gaussian made on average only a 2.2% difference.

Contraction histograms

The histograms of polarized fluorescence fluctuations obtained from contracting myofibrils were significantly different from those observed in rigor and relaxation. Fig. 6 shows examples of six histograms of polarized fluorescence randomly selected from a pool of 20 histograms of contracting myofibrils. The average skewness and kurtosis were 0.86 ± 0.16 (SD) and −0.59 ± 0.27 (SD), respectively. Both skewness and kurtosis were statistically significantly different during rigor and contraction at a level of 0.69% for skewness ($t = -2.87$, $P = 0.0069$, 34 degrees of freedom) and at a level of <0.07% for kurtosis ($t = -3.68$, $P = 0.00078$, 34 degrees of freedom), respectively. The standard error test of the PeakFit program showed that 14 of 20 histograms were best fit by two Gaussians. The average positions of the peaks were $P = -0.14 \pm 0.04$ for peak 1 and $P = -0.31 \pm 0.05$ for peak 2 (Table 2). The positions of the two peaks were significantly statistically different at $P < 0.001\%$ ($t = 9.92$). Most of the power was contained in peak 1, although on two occasions the peak 2 was larger than peak 1 (e.g., Fig. 6, *right upper corner*). The average ratio, i.e., the relative contribution of both Gaussians, was 5.7 ± 7.7. The overall experimental curve (*blue*) is the sum of the red (peak 1) and green (peak 2) Gaussians.

Reversibility

To ensure that the second Gaussian peak observed during contraction was not an artifact induced by the contraction protocol itself, we examined the orientational distributions in rigor before and after contraction of the myofibrils. Histograms of fluctuations in naive rigor myofibrils examined immediately after preparation were compared with histograms from myofibrils that had first contracted and then returned to rigor. The contribution of the second peak was

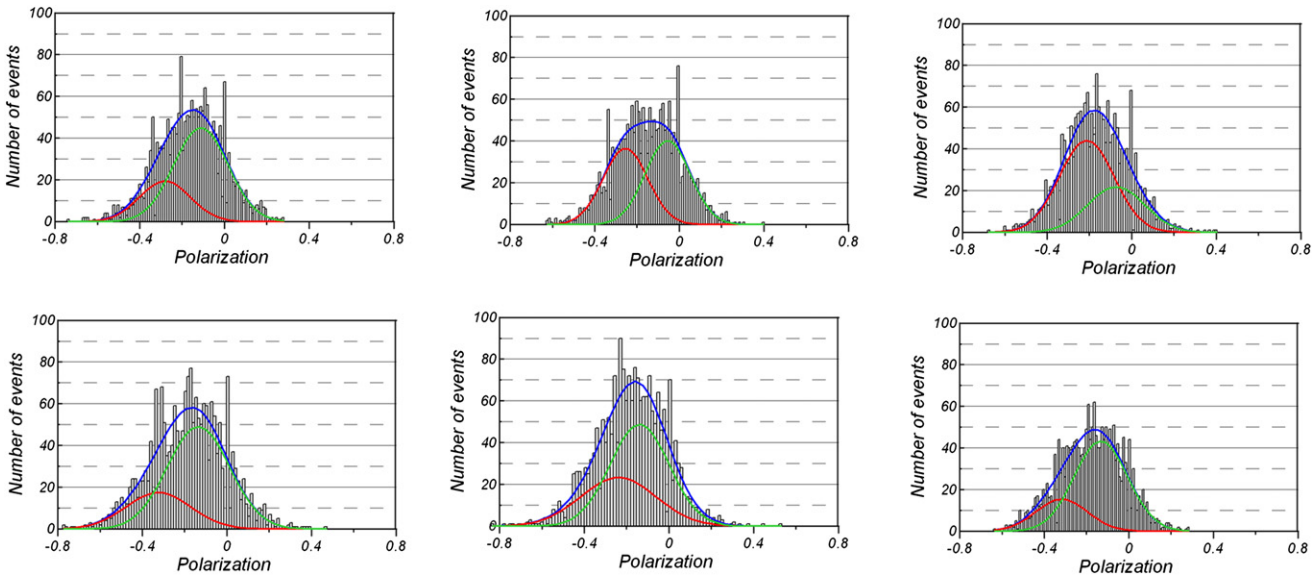

FIGURE 6 Examples of histograms of polarized fluorescence from contracting myofibrils. Horizontal scale: The negative value of fluorescence polarization. Vertical scale: The number of events during 20 s. The positions of minor (*red line*) and major (*green line*) peaks from a double Gaussian distribution fit are (clockwise from the top left) $P = -0.3$ and 0.11, $P = -0.29$ and −0.06, $P = -0.2$ and −0.06, $P = -0.33$ and −0.14, $P = -0.32$ and −0.11, and $P = -0.31$ and .012. The ratios of the major peak (*green line*) to the corresponding minor peak (*red line*) in the double Gaussian fits are (clockwise, from the top left corner) 2.7, 1.1, 0.5, 2.7, 1.6, and 3.1. The blue line is the sum of red and green line fits.

TABLE 2 Average polarization values from the Gaussian distribution fits

Myofibrils	Peak 1	Peak 2	*N*
Rigor	0.04 ± 0.02	-	18
EDC-rigor	0.05 ± 0.08	-	20
Relaxation	−0.03 ± 0.03	-	18
EDC-relaxation	−0.06 ± 0.02	-	18
Contraction	−0.14 ± 0.04	−0.31 ± 0.05	16*

Errors are given as SD, and *N* is the number of experiments.
*A total of 20 histograms were analyzed, and four of these were best fit by a single Gaussian distribution with the peak position corresponding to that reported by peak 1.

small in both rigor cases (2.6 and 8.8%, respectively; Fig. S5) in comparison with contracting myofibrils (51%; Fig. S6).

DISCUSSION

The main finding of this study is that polarization histograms from fluorescently labeled LC1 on the myosin head during muscle contraction consist of two separate peaks. Because the peaks correspond to the number of times a cross-bridge assumes a given orientation during 20 s of contraction, it makes sense to suggest that during contraction, cross-bridges assume two distinct orientations. There was a large difference in polarization between the two peaks. They most likely indicate cross-bridge conformations in the pre-and post-power-stroke positions. The first peak corresponds to the pre-power-stroke position; the cleft between the upper and lower subdomains of the 50 KDa fragment is partially closed, the lever arm is in the up orientation and the myosin active site contains ADP and Pi (5). The second peak corresponds to the post-power-stroke position when the cleft between the upper and lower subdomains of the 50 KDa fragment is totally closed, the lever arm is in the partially down orientation and the myosin active site contains only ADP (5). The area corresponds to the average number of times a cross-bridge assumes a given orientation during the 20 s contraction, and the average ratio of the area under peak 1 divided by the area under peak 2 was 5.7. Therefore, the fact that the pre-power-stroke state is more populated than the post-power-stroke state is consistent with the notion that the transition from the pre- to the post-power stroke is rate-limiting.

In a previous study, Ostap et al. (9) used EPR spectroscopy to detect ATP-induced changes in the structure of spin-labeled myosin heads in whole muscle fibers in rigor upon transition to relaxation and contraction. Different conformational states were resolved on the basis of nanosecond rotational motion within the protein. In rigor, only a single conformation was detected, in agreement with the findings presented here. In relaxation and isometric contraction, the EPR spectrum showed two conformations and a small fraction of heads in the oriented, actin-bound conformation. Ostap et al.'s rigor results are consistent with those reported here; however, the relaxation and contraction results differ, most likely because they used whole muscle fibers labeled at Cys-707, whereas we observed three cross-bridges labeled at LC1 in myofibrils. Ling et al. (12) and later Hopkins et al. (25) studied the breadth of the orientation distribution of fluorescent probes bound to the regulatory light chain of myosin, and found that it was essentially the same in different physiological states. This result is consistent with our study, which also did not show consistent changes in the width of distributions.

In our experiments, the post-power-stroke conformation of the lever arm is different from the rigor conformation. This implies that each cross-bridge executes a rotation in two steps. Fig. 7 illustrates schematically the presumed

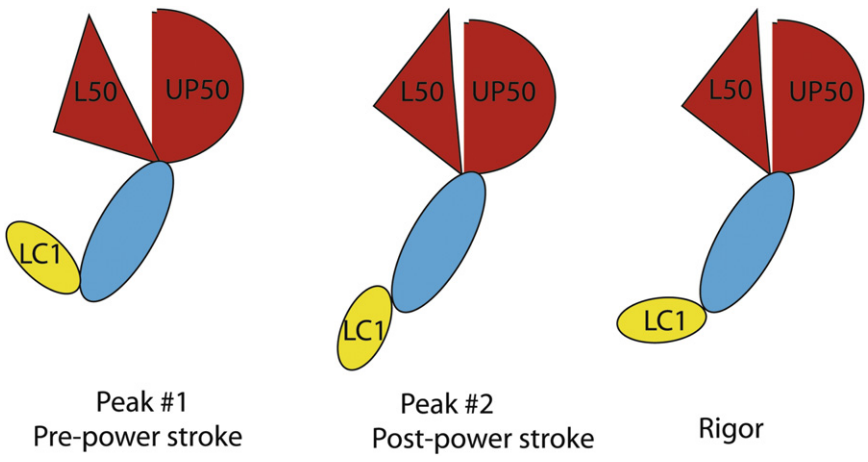

FIGURE 7 Schematic illustration of the cross-bridge power stroke. In the pre-power-stroke state, corresponding to peak 1 of the polarized fluorescence histograms from contracting myofibrils, the upper and lower 50 K domains (UP50 and L50; notation as in Coureux et al. (5)) are in a partially closed conformation and LC1 is pointing sidewise (low polarization). In the post-power-stroke state, corresponding to peak 2 of the polarized fluorescence histograms from contracting myofibrils, the upper and lower 50 K domains are in a closed conformation and LC1 is pointing downward (high polarization). The rigor state is short-lived and the myosin head adopts a conformation similar to that of the post-power-stroke state (5) except that LC1 is now pointing completely sideways (zero polarization). This schematic does not take into account such complicating factors as disorganization of actin filaments and inhomogeneities between myofibrils. For simplicity, it is assumed that the transition dipole of rhodamine is parallel to the long axis of LC1.

sequence of events. A cross-bridge is initially in the pre-power-stroke state, represented by peak 1, and subsequently transits to the post-power-stroke state (weak ADP binding state), represented by peak 2. If the rigor state (strong interaction of the apo-head with actin) is a part of the cross-bridge cycle, there must be a second transition from the post-power-stroke state to the rigor state. The rigor conformation is not seen during contraction because this state is short-lived in the presence of excess ATP. This interpretation is consistent with the model originally proposed by Huxley and Simmons (33), which suggests that the myosin head has a small number of sites, each of which is capable of combining reversibly with a corresponding site on F-actin.

We did not attempt to translate the polarization values to the absolute orientation of transition dipoles with respect to the myofibrillar axis, because this orientation is critically dependent on the model used to arrange the cross-bridges. For example, if it is assumed that the cross-bridges are arranged helically along the long axis of muscle and the fluorescence contains α% contribution from a random, immobilized component, the difference between the pre- and post-power-stroke angles will correspond to an angular change from 90° to 5° depending on the value of α (22). However, by calculating the average area under the Gaussian curves, we can estimate that the relative populations of cross-bridges are ~70% in the pre-power-stroke states and ~30% in the post-power-stroke states.

An additional possibility is that the two different peaks indicate two populations of cross-bridges, each of which executes a distinct rotation. This is unlikely, however, because the presence of two populations was not detected in direct electron microscopy measurements of cryofixed, isometrically active, insect flight muscle (13). It is also possible that cross-bridges do not rotate at all during isometric contraction, and our results reflect their static arrangement. In the absence of filament sliding, cross-bridges may not be able to rotate while attached, and cross-linking may prevent them from reaching neighboring actin target zones while detached (13). This interpretation does not alter the conclusions of this study. The observed distributions would then correspond to static positions that were assumed after the first molecule of ATP was split when a cross-bridge was still allowed to rotate against an unstretched elastic element.

We want to emphasize that, in contrast to previous studies (e.g., Muthu et al. (26)), we did not perform a correlation analysis of the kinetic data. This is a significant advantage of our method because a correlation analysis requires assumptions about a model of cross-bridge-actin interaction.

We considered three possible artifacts, as described below, and concluded that all are unlikely:

1. The second peak is due to rotation of the rhodamine moiety alone. Although the mobile fraction was 10% (Fig. 3 *B*), this is unlikely because 1), rotational motion on a scale of nanoseconds does not affect polarization of fluorescence measured on a scale of milliseconds; and 2), the nanosecond rotation of rhodamine is clearly visible in a solution of free dye (Fig. 3), whereas the second peak is not visible in rigor myofibrils (Fig. 5).
2. Addition of ATP alone is sufficient to induce the appearance of the peaks. However, in control experiments we saw no effect of ATP on the anisotropy or fluorescent lifetime of rhodamine-LC1.
3. The fluctuations are caused by myofibril movement, not cross-bridge rotations. This is unlikely because the control experiments, in which we measured sarcomere length as a function of the concentration of cross-linker, showed no shortening upon addition of ATP when myofibrils were cross-linked with 20 mM EDC.

SUPPORTING MATERIAL

Six figures are available at http://www.biophysj.org/biophysj/supplemental/S0006-3495(11)00052-X.

This work was supported by grants from the National Institutes of Health (R01AR048622 and R01HL090786).

REFERENCES

1. Geeves, M. A., and K. C. Holmes. 2005. The molecular mechanism of muscle contraction. *Adv. Protein Chem.* 71:161–193.
2. Houdusse, A., and H. L. Sweeney. 2001. Myosin motors: missing structures and hidden springs. *Curr. Opin. Struct. Biol.* 11:182–194.
3. Ferenczi, M. A., S. Y. Bershitsky, …, A. K. Tsaturyan. 2005. The "roll and lock" mechanism of force generation in muscle. *Structure.* 13:131–141.
4. De La Cruz, E. M., and E. M. Ostap. 2009. Kinetic and equilibrium analysis of the myosin ATPase. *Methods Enzymol.* 455:157–192.
5. Coureux, P. D., H. L. Sweeney, and A. Houdusse. 2004. Three myosin V structures delineate essential features of chemo-mechanical transduction. *EMBO J.* 23:4527–4537.
6. Sakamoto, T., M. R. Webb, …, J. R. Sellers. 2008. Direct observation of the mechanochemical coupling in myosin Va during processive movement. *Nature.* 455:128–132.
7. Sellers, J. R., and C. Veigel. 2010. Direct observation of the myosin-Va power stroke and its reversal. *Nat. Struct. Mol. Biol.* 17:590–595.
8. Walker, M. L., S. A. Burgess, …, P. J. Knight. 2000. Two-headed binding of a processive myosin to F-actin. *Nature.* 405:804–807.
9. Ostap, E. M., V. A. Barnett, and D. D. Thomas. 1995. Resolution of three structural states of spin-labeled myosin in contracting muscle. *Biophys. J.* 69:177–188.
10. Thomas, D. D., and R. Cooke. 1980. Orientation of spin-labeled myosin heads in glycerinated muscle fibers. *Biophys. J.* 32:891–906.
11. Borejdo, J., O. Assulin, …, S. Putnam. 1982. Cross-bridge orientation in skeletal muscle measured by linear dichroism of an extrinsic chromophore. *J. Mol. Biol.* 158:391–414.
12. Ling, N., C. Shrimpton, …, M. Irving. 1996. Fluorescent probes of the orientation of myosin regulatory light chains in relaxed, rigor, and contracting muscle. *Biophys. J.* 70:1836–1846.
13. Tregear, R. T., M. C. Reedy, …, M. K. Reedy. 2004. Cross-bridge number, position, and angle in target zones of cryofixed isometrically active insect flight muscle. *Biophys. J.* 86:3009–3019.

14. Sabido-David, C., B. Brandmeier, …, M. Irving. 1998. Steady-state fluorescence polarization studies of the orientation of myosin regulatory light chains in single skeletal muscle fibers using pure isomers of iodoacetamidotetramethylrhodamine. *Biophys. J.* 74:3083–3092.

15. Hopkins, S. C., C. Sabido-David, …, Y. E. Goldman. 1998. Fluorescence polarization transients from rhodamine isomers on the myosin regulatory light chain in skeletal muscle fibers. *Biophys. J.* 74:3093–3110.

16. Kraft, T., T. Mattei, …, B. Brenner. 2002. Structural features of crossbridges in isometrically contracting skeletal muscle. *Biophys. J.* 82:2536–2547.

17. Burghardt, T. P., T. Ando, and J. Borejdo. 1983. Evidence for crossbridge order in contraction of glycerinated skeletal muscle. *Proc. Natl. Acad. Sci. USA.* 80:7515–7519.

18. Qian, H., S. Saffarian, and E. L. Elson. 2002. Concentration fluctuations in a mesoscopic oscillating chemical reaction system. *Proc. Natl. Acad. Sci. USA*. 99:10376–10381.

19. Dos Remedios, C. G., R. G. Millikan, and M. F. Morales. 1972. Polarization of tryptophan fluorescence from single striated muscle fibers. A molecular probe of contractile state. *J. Gen. Physiol.* 59:103–120.

20. Dos Remedios, C. G., R. G. Yount, and M. F. Morales. 1972. Individual states in the cycle of muscle contraction. *Proc. Natl. Acad. Sci. USA*. 69:2542–2546.

21. Nihei, T., R. A. Mendelson, and J. Botts. 1974. Use of fluorescence polarization to observe changes in attitude of S-1 moieties in muscle fibers. *Biophys. J.* 14:236–242.

22. Tregear, R. T., and R. A. Mendelson. 1975. Polarization from a helix of fluorophores and its relation to that obtained from muscle. *Biophys. J.* 15:455–467.

23. Morales, M. F. 1984. Calculation of the polarized fluorescence from a labeled muscle fiber. *Proc. Natl. Acad. Sci. USA*. 81:145–149.

24. Sabido-David, C., S. C. Hopkins, …, M. Irving. 1998. Orientation changes of fluorescent probes at five sites on the myosin regulatory light chain during contraction of single skeletal muscle fibres. *J. Mol. Biol.* 279:387–402.

25. Hopkins, S. C., C. Sabido-David, …, Y. E. Goldman. 2002. Orientation changes of the myosin light chain domain during filament sliding in active and rigor muscle. *J. Mol. Biol.* 318:1275–1291.

26. Muthu, P., P. Mettikolla, …, J. Borejdo. 2010. Single molecule kinetics in the familial hypertrophic cardiomyopathy D166V mutant mouse heart. *J. Mol. Cell. Cardiol.* 48:989–998.

27. Borejdo, J., D. Szczesna-Cordary, …, N. Calander. 2010. Familial hypertrophic cardiomyopathy can be characterized by a specific pattern of orientation fluctuations of actin molecules. *Biochemistry.* 49:5269–5277.

28. Herrmann, C., C. Lionne, …, T. Barman. 1994. Correlation of ActoS1, myofibrillar, and muscle fiber ATPases. *Biochemistry.* 33:4148–4154.

29. Tsaturyan, A. K., S. Y. Bershitsky, …, M. A. Ferenczi. 1999. Structural changes in the actin-myosin cross-bridges associated with force generation induced by temperature jump in permeabilized frog muscle fibers. *Biophys. J.* 77:354–372.

30. Borejdo, J., P. Muthu, …, T. P. Burghardt. 2007. Rotation of actin monomers during isometric contraction of skeletal muscle. *J. Biomed. Opt.* 12:014013.

31. Magde, D., E. L. Elson, and W. W. Webb. 1974. Fluorescence correlation spectroscopy. II. An experimental realization. *Biopolymers.* 13:29–61.

32. Elson, E. L. 2007. Introduction to FCS. *In* Short Course on Cellular and Molecular Fluorescence, *Vol. 2*. Z. Gryczynski, editor. University of North Texas, Fort Worth. 1–10.

33. Huxley, A. F., and R. M. Simmons. 1971. Proposed mechanism of force generation in striated muscle. *Nature.* 233:533–538.